Original Article

Prediction of prostate cancer recurrence after radiation therapy using multiparametric magnetic resonance imaging and spectroscopy: assessment of prognostic factors on pretreatment imaging

Audrey Asuncion[1]^, Paul Michael Walker[2,3], Aurélie Bertaut[4], Julie Blanc[4], Maxime Labarre[5], Etienne Martin[6], Florian Bardet[7], Jeremy Cassin[1], Luc Cormier[7], Gilles Crehange[8], Romaric Loffroy[1,3]^, Alexandre Cochet[2,3,9]

[1]Department of Diagnostic & Interventional Radiology, University Hospital Dijon, Dijon, France; [2]Department of Spectroscopy and Nuclear Magnetic Resonance, University Hospital Dijon, Dijon, France; [3]Laboratory of Imaging and Artificial Vision (ImVIA), IFTIM Team, EA 7535, University of Burgundy, Dijon, France; [4]Department of Methodology and biostatistics, Centre Georges-François-Leclerc, Dijon, France; [5]Department of Radiology, Centre Georges-François-Leclerc, Dijon, France; [6]Department of Radiotherapy, Centre Georges-François-Leclerc, Dijon, France; [7]Department of Urology, University Hospital Dijon, Dijon, France; [8]Department of Radiotherapy, Institut Curie, Paris, France; [9]Department of Nuclear Medicine, Centre Georges-François-Leclerc, Dijon, France

Contributions: (I) Conception and design: G Crehange, A Cochet, PM Walker; (II) Administrative support: A Cochet, PM Walker, A Asuncion; (III) Provision of study materials or patients: PM Walker, G Crehange; (IV) Collection and assembly of data: M Labarre, PM Walker, A Asuncion; (V) Data analysis and interpretation: M Labarre, PM Walker, A Asuncion; (VI) Manuscript writing: All authors; (VII) Final approval of manuscript: All authors.

Correspondence to: Audrey Asuncion. Department of Radiology, University Hospital Dijon, 1 rue du Professeur Marion, 21000 Dijon, France. Email: audreyasuncion@aol.com.

Background: To assess whether data from pre-therapeutic multiparametric magnetic resonance imaging (mpMRI) combined with three-dimensional magnetic resonance spectroscopy (3D MRS) provide prognostic factors of biochemical relapse in patients with localized prostate cancer treated by external radiotherapy or brachytherapy.

Methods: In our single institution observational retrospective study we included a cohort of 230 patients treated by external radiotherapy or brachytherapy who had an initial mpMRI with 3D MRS from January 2008 to December 2015 for newly diagnosed localized prostatic cancer, proven histologically. Three trained radiologists recorded tumor characteristics, MRI T-stage and metabolic abnormalities from 3D MRS data. Univariate and multivariate Cox analyzes explored the relationship between clinical and imaging variables to highlight prognostic factors for recurrence, using biochemical relapse as the primary endpoint.

Results: mpMRI data analysis allowed to reclassify 21.7% of the patients in a MRI National Comprehensive Cancer Network (NCCN) group higher than their initial clinical T-stage, but also to detect a lesion in 78% of the patients considered as clinically T1c. After a median of follow-up of 8.7 years (IQR, 6.6–10.1) following cancer diagnosis, 36 (16%) patients developed a biochemical relapse. The multivariate Cox analysis demonstrated the existence of 3 independent factors for prediction of biochemical recurrence: extracapsular extension (ECE) (HR =3.33; 95% CI: 1.93–5.73; P<0.01), choline/citrate ratio in healthy tissue in the transition zone (TZ) (HR =2.96; 95% CI: 1.06–8.28; P=0.04) and the NCCN Magnetic Resonance Imaging classification (intermediate versus low-risk, HR =3.06; 95% CI: 1.13–8.30; P<0.01).

^ ORCID: Audrey Asuncion, 0000-0002-1516-8952; Romaric Loffroy, 0000-0002-3107-5967.

© Quantitative Imaging in Medicine and Surgery. All rights reserved.

Conclusions: Combination of mpMRI and 3DMRS could aid in the prognostic stratification of localized prostate cancer treated by radiotherapy or brachytherapy, by combining accurate evaluation of tumor extension, and quantification of prostate metabolism.

Keywords: Prostate; cancer; magnetic resonance imaging (MRI); spectroscopy; radiotherapy

Submitted Mar 26, 2022. Accepted for publication Aug 22, 2022.
doi: 10.21037/qims-22-184
View this article at: https://dx.doi.org/10.21037/qims-22-184

Introduction

The standard of care for patients with localized prostate cancer relies on surgery, external beam radiotherapy (EBRT) or brachytherapy (BT), based on the work of D'Amico and colleagues (1) and on the recommendations from the National Comprehensive Cancer Network (NCCN) (2) in which the patient is classified.

However, despite this rigorous classification and therefore the choice of appropriate treatment, more than half of the patients will experience a biochemical relapse within 10 years (3,4). Thus, due to the low sensitivity (33%) and high inter-observer variability of the digital rectal examination (5,6), multiparametric magnetic resonance imaging (mpMRI) has been playing an increasingly important role in diagnosis, including the detection of tumor location (83%) for patients with prostate specific antigen (PSA) levels indicative of cancer, but with negative biopsy results (7) or more recently to guide biopsies (8). Furthermore, the literature has shown its major interest in the establishment of the tumor stage (9,10) particularly in the detection of extracapsular extension (ECE) or seminal vesicle involvement (11-13). Moreover, the Prostate Imaging-Reporting and Data System version 2.1 (PI-RADSv2.1) initially developed as a diagnostic tool for significant prostate cancer (14) has shown its interest as an independent predictor of the risk of biochemical recurrence (15,16).

On the other hand, 3D magnetic resonance spectroscopy (MRS) makes it possible to study the entire prostate metabolism, and more specifically that of a tumor lesion. Combined with mpMRI, it has shown some promise in the detection of cancer on 3Tesla mpMRI (17,18). In Scheidler's work (19) on tumor localization, the addition of 3D MRS fared better than mpMRI alone, with 90% specificity and 50% sensitivity. In addition, 3D MRS has shown interest in the evaluation of ECE, tumor volume on initial mpMRI (20) or in the improvement of biopsy yield (21). Other studies have also brought to light the benefit of combining mpMRI and spectroscopy to detect residual disease or local recurrence by the persistence of a metabolic profile, especially for patients treated by EBRT (22,23).

Nevertheless, whilst the T-stage defined on mpMRI or PI-RADS v2 can better predict the prognosis of patients after radiotherapy, the use in the NCCN risk group classification remains uncertain. Indeed, the prognostic value of mpMRI was studied in series after surgery where the Gleason score and T-stage were established on the radical prostatectomy specimen (24).

To our knowledge, after EBRT, few studies have been able to establish prognostic factors for recurrence—when using mpMRI, and especially concerning the potential contribution of 3D MRS data.

Therefore, we undertook this study to evaluate whether pretreatment combined pelvic mpMRI and 3D MRS findings are predictive of biochemical relapse, in patients who undergo EBRT or BT for localized prostate cancer. We present the following article in accordance with the STROBE reporting checklist (available at https://qims.amegroups.com/article/view/10.21037/qims-22-184/rc) (25).

Methods

Design and population

Between January 2008 and December 2015, 1,300 prostate cancer patients underwent mpMRI at 3T using the same protocol in our institution the University Hospital of Dijon, France.

Patients were retrospectively selected in this observational study using the following inclusion criteria:

(I) Prostate cancer confirmed by sextant biopsies and diagnosed between January 2008 and December 2015; radiotherapy or BT treatment delivered with respect to D'Amico classification and international recommendations (1);

© Quantitative Imaging in Medicine and Surgery. All rights reserved.

(II) At least 5 years of PSA follow-up after completion of radiation.

Patients were excluded if they had radical prostatectomy, hormonal or any other form of local therapy before their EBRT or BT, pelvic lymph node or metastases (rectal, bladder, bone…), absence of entire PSA follow-up, absence of pre-therapeutic mpMRI or poor quality mpMRI (metal artifact mainly related to total hip prothesis, patient movement or digestive gas, incomplete mpMRI) with impossible interpretation.

A clinical examination was performed before the mpMRI in all patients, allowing a T-tumor classification according to the International Union Against Cancer (UICC) (26) as well as an ultrasound-guided transrectal prostate biopsy and at least one blood PSA level test, in accordance with international recommendations (2). Patients were then classified according to the D'Amico and the NCCN classification systems (national and international classification based on T-stage, Gleason score and initial PSA level) to adapt work-up and treatment.

Indeed, after discussion on a multidisciplinary tumor board and with respect to the D'Amico classification according to the international recommendations (27), each patient was treated either by EBRT, prostate BT, or both. EBRT was delivered by a dose escalated intensity-modulated technique. Exclusive and BT boost is enabled by the intra-prostatic introduction of permanent radioactive iodine seeds (low-dose rate technique, LDR).

Patients were followed by their radiation oncologist, within 3 months after the completion of radiation, and every 6 months thereafter for 5 years as well as annual consultations over 5 years. A PSA blood sample was taken every 6 months during a follow-up period of 5 years at least, up to 10 years of follow-up or more for 49 patients.

According to the Phoenix definition, biochemical recurrence was defined as an increased PSA level with nadir + 2 ng/mL (28).

All initial clinical and biological data were recorded from the medical record patient. The study was conducted in accordance with the Declaration of Helsinki (as revised in 2013). The study was approved by the ethics committee of the University Hospital of Dijon and individual consent for this retrospective analysis was waived.

MRI technique and MRS

All patients had a baseline mpMRI on a 3T whole body magnet (Siemens Magnetom Trio TIM, Erlangen, Germany) using a pelvic multichannel phased-array coil (eight channels) as described previously (29).

Each mpMRI included at least one 3D T2 turbo spin echo (T2 TSE) volumetric sequence and two functional sequences including diffusion-weighted images (DWI) using two values of b (b200–b800) and dynamic contrast enhanced (DCE) T1-weighted images allowing the realization of perfusion curves and the study of the wash-in dynamics (protocol meeting international recommendations) (30-32) Indeed, these imaging modalities are the main stay of the prostate imaging protocol and feature regularly in publications (33,34).

A 3-mm-slice T2-weighted fast spin-echo sequence with a nominal pixel size of 0.9 mm (repetition time, 3,400 ms; echo time 85 ms; and echo train length, 13) was used to acquire images in oblique, sagittal, and coronal planes oriented parallel to the prostate peripheral zone (PZ)-rectal wall axis. 3D T2-weighted fast spin-echo (repetition time 3,000 ms; echo time 143 ms; echo train length, 109; and slice thickness, 1.5 mm) images were then acquired in an oblique axial plane oriented perpendicular to the prostate PZ rectal wall axis. The nominal matrix and field of-view of the 3D T2-weighted images were respectively 384×308 and 280×240 mm^2, thereby affording submillimetric pixel resolution within the imaging plane. This same image acquisition protocol was used for all patients of the cohort.

Three-dimensional proton MRS was performed by using a water- and lipid-suppressed double spin-echo point-resolved spectroscopic sequence (PRESS). The volume for MRS was selected to maximize coverage of the prostate while minimizing inclusion of rectal air and periprostatic fat.

A representative slice (or series of slices) was chosen for each tumor on the 3D T2 sequence and the concentrations (in mmol/L) of choline and citrate were reported in a number of voxels located in tumor and healthy tissue. The actual number of voxels studied depended on the tumor tissue volume. The data collection was carried out in both transition zone (TZ) and PZ for each patient (an example is presented in *Figure 1*). Ratios for choline to citrate (Cho/Cit) were also automatically calculated for every voxel.

The MRI parameters studied were: the size (mm) and volume of the prostate (mL) and the number of tumors (lesions classified PI-RADS 3 to 5). In healthy tissue, the apparent diffusion coefficient (ADC in mm^2/s) and wash-in calculation from DCE-MRI (directing coefficient of the ascending slope) were measured in healthy prostate PZ and in healthy TZ tissues.

© Quantitative Imaging in Medicine and Surgery. All rights reserved.

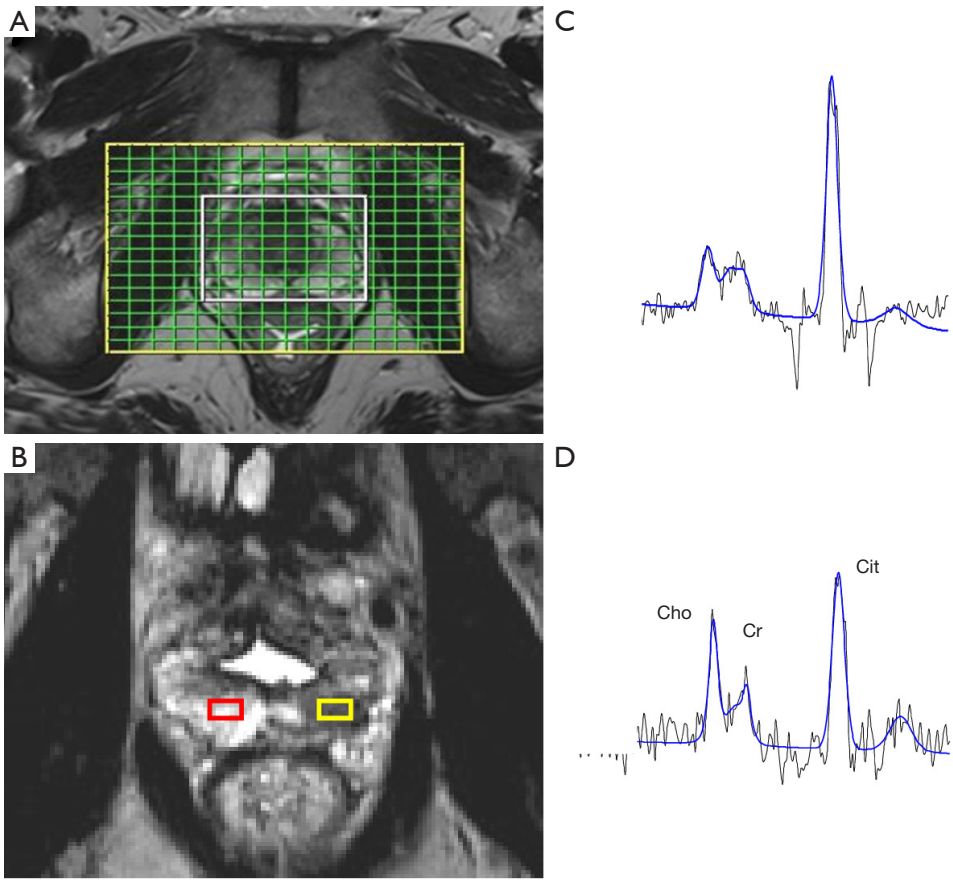

Figure 1 Example of 3D MRS imaging. (A) The 3D MRS grid is positioned around the whole prostate on T2-weighted images. (B) Two voxels are seen here positioned on a T2-weighted image within normal PZ prostate tissue (red box) and PZ cancer tissue (yellow box). (C) Spectrum from normal PZ prostate and (D) spectrum from cancer tissue. The metabolites present in the spectra are Cho, Cr and Cit. 3D MRS, three-dimensional magnetic resonance spectroscopy; PZ, peripheral zone; Cho, choline; Cr, creatine; Cit, citrate.

For each tumor lesion visualized, several parameters were studied: the largest tumor size in T2 TSE (mm), the location (apex, middle, base on PZ, TZ or anterior fibromuscular stroma), the presence of ECE and its length (mm), tumor ADC (mm^2/s) and size (mm) at b800 on DWI, the average of the lowest 10% of ADCs within the lesion, tumor perfusion wash-in coefficient, tumor perfusional curve classified from 1 to 3.

To estimate presence of ECE, the readers used the European Society of Urogenital Radiology (ESUR) criteria (30).

Finally, each lesion was classified according to its MRI tumor stage and the PI-RADS v2.1 score (from 1 to 5) allowing patients to be ranked according to their risk of recurrence using the D'Amico-MRI and NCCN-MRI classifications. Indeed, by replacing the clinical T-stage by the MRI T-stage, we created the D'Amico-MRI and NCCN-MRI classifications, respectively. Then we compared the risk group difference between the clinical classifications (NCCN and D'Amico) and their counterpart obtained after mpMRI analysis.

A senior radiologist (with more than 13 years of experience), who was trained in an expert center (that performs a minimum of 400 prostate mpMRI per year) evaluated all mpMRI images.

Two younger radiologists in mpMRI prostate training, independently, blinded from the first report and from the patient's treatment and follow-up, also assessed the mpMRI.

The image analysis was performed with Syngo.via software and ImageJ software.

Statistical analysis

Dichotomous or categorical variables were described by their

© Quantitative Imaging in Medicine and Surgery. All rights reserved.

Table 1 Clinical and demographics characteristics

Characteristics	Value
Age at diagnostic (years)	68.0 [62.0–72.0]
Clinical T-stage	
T1c	119 (51.7)
T2a	34 (14.8)
T2b	35 (15.2)
T2c	22 (9.6)
T3a	19 (8.3)
T3b	1 (0.4)
ISUP grade	
1	150 (65.2)
2: 3+4	50 (21.7)
3: 4+3	20 (8.7)
5	4 (1.7)
Pre-treatment PSA (ng/mL)	7.5 [5.5 – 11.5]
Clinical based D'Amico risk group	
Low	99 (43.0)
Intermediate	82 (35.7)
High	49 (21.3)
Clinical based NCCN risk group	
Low	99 (43.0)
Intermediate	29 (12.6)
High	97 (42.2)
Very high	5 (2.2)
Treatment	
EBRT	106 (46.0)
EBRT + HT	43 (18.8)
BT	72 (31.3)
BT + HT	1 (0.4)
EBRT + BT	7 (3.1)
EBRT + BT + HT	1 (0.4)
Post treatment PSA nadir (ng/mL)	0.2 [0.1–0.4]
Survival status	
Alive	201 (87.4)
Dead	29 (12.6)
Disease-related death	1 (3.7)
Biochemical relapse	37 (16.1)
Recurrence site	
Local (prostate)	22 (59.5)
Metastatic (rectal, bone, etc.)	10 (27.0)
Regional (N+)	4 (10.8)
Unknown	1 (2.7)
Years between diagnostic and biochemical relapse	6.0 [4.6–8.0]

All parameters are median [Q1–Q3] or number (percentage). N=230. ISUP, International Society of Urological Pathology; PSA, prostatic specific antigen; NCCN, National Comprehensive Cancer Network; EBRT, external beam radiotherapy; HT, hormonotherapy; BT, brachytherapy.

frequency (percentage) and compared using the Chi-square of Fisher test. Continuous variables were described as mean with standard deviation (SD) and as median with interquartile range (IQR) and compared using Student's *t*-test or Wilcoxon test. Biochemical relapse-free survival was defined as the time between diagnosis and biochemical relapse or death. Patients alive without biochemical relapse were censored on the date of the last follow-up. Survival curves were obtained using the Kaplan-Meier method. Independent correlates of biochemical free relapse were determined in multivariate Cox regression models. As NCCN-MRI, PI-RADS v2 and ECE are highly correlated, three different models have been used with these independent variables. We removed from the multivariate model, patients with missing data for one of the variables of interest in the multivariate analysis. Variables eligible for multivariate analyses were selected from univariate analyses with a threshold to enter the multivariate model of 0.20 and no more than 15% of missing data. The final models include all significant variables at the threshold of 0.10. Harrell's Coefficient was calculated for each multivariate analysis. All tests were two-sided, P values less than 0.05 were considered as significant. Analyses were performed using SAS 9.4.

Results

Description of the population

All initial clinical and biological data were recorded from the medical record patient, described in *Table 1*. The flow chart of the study is represented in *Figure 2*.

Two hundred and thirty [230] patients were included

© Quantitative Imaging in Medicine and Surgery. All rights reserved.

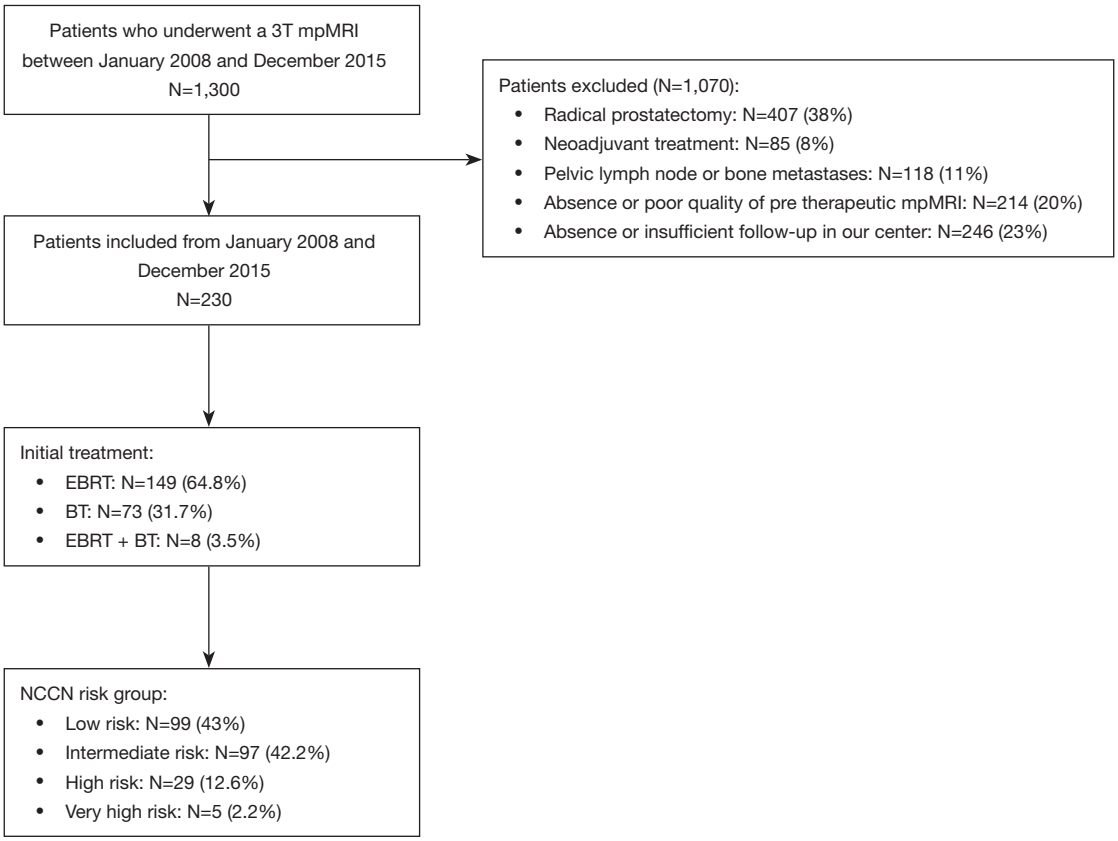

Figure 2 Flow chart of the study. 3T, 3 Tesla; mpMRI, multiparametric magnetic resonance imaging; EBRT, external beam radiotherapy; BT, brachytherapy; NCCN, National Comprehensive Cancer Network.

in this study, the mean (SD) age at diagnosis was 67.5 (6.7) years. They were all followed completely over at least 5 years and the median total duration of follow-up was 8.7 years (IQR, 6.6–10.1 years).

According to D'Amico classification, 99 (43%) patients were classified as low risk, 82 (35.7%) as intermediate risk and 49 (21.3%) as high risk.

Similarly, for the NCCN classification, 99 (43%) patients were classified as low risk, 97 (42.2%) as intermediate risk, 29 (12.6%) as high risk and 5 (2.2%) as very high risk.

Seventy-three [73] patients underwent permanent implants with iodine seeds as monotherapy, 157 patients received EBRT, including 8 with BT boost as a complement. The 149 patients, treated with EBRT only, received a median total dose of 78 Gray (Gy) (IQR, 72–80 Gy) and the 8 with a BT boost complement a median total dose of 156 Gy (IQR, 156–157 Gy). Forty-four [44] patients (19%) had a complementary androgen deprivation therapy in combination treatment.

In this study, the 37 (16%) patient with observed biochemical recurrence were composed of 45.9% Gleason 6 (versus 68.9% in the group without recurrence) and with significantly higher Gleason scores: 40.5% of Gleason 7 (versus 28.5%), 5.4% of Gleason 8 (versus 0.5%), 5.5% of Gleason 9 or 10 (versus 1%) (P=0.06). Indeed, patients who relapsed had significantly more often a Gleason score ≥7 (51.4% versus 30.1%; P<0.01) and higher initial clinical T-stage (10.8% T2c versus 9.3%, 18.9% T3a versus 6.2%, 2.7% T3b versus 0%; P=0.04) than those who did not.

mpMRI and spectroscopic analyses

All mpMRI were performed after the histological diagnostic of cancer and before any treatment.

The median prostatic volume on mpMRI was 46.7 mL (IQR, 37.5–62.5 mL). One hundred and eighty-seven [187] patients had a single lesion identifiable by mpMRI, 15 had two visible lesions (the most unfavorable PI-RADS of the

© Quantitative Imaging in Medicine and Surgery. All rights reserved.

two was retained for the patient global score) and 29 had no visible lesion (lesions that were not detectable were classified as PI-RADS 1/5 or 2/5, namely benign lesions). A total of 217 lesions were therefore detected on mpMRI.

Finally, 106 patients were classified PI-RADS 5/5, 70 PI-RADS 4/5 and 26 PI-RADS 3/5.

A comparison of mpMRI parameters among patients with or without biochemical relapse is shown in *Table 2*. Patients with biochemical relapse had larger tumor size (P<0.01) and longer capsular contact length of the tumor (P<0.01) when compared with patients without. Moreover, they more often had 2 lesions detected (P=0.03), and ECE (P<0.01). Patients with biochemical relapse also had slightly lower ADC value of the tumor, and higher wash-in coefficient (P=0.04 for both).

There was no significant difference concerning the extension to seminal vesicles (P=0.2), nor with the spectroscopic data, notably with the increase in the Cho/Cit ratio for tumors in the PZ (P=0.6). Initial spectroscopic analyses are presented in Table S1.

Evolution of prognostic groups after mpMRI

Firstly, the analysis of the comparison between clinical T-stage and MRI T-stage showed that after mpMRI 128 (55%) patients moved to a higher MRI T-stage. Seventy eight (34%) patients did not change their stage and 24 (10.4%) moved to a lower MRI T-stage than their clinical T-stage.

The same was true for the comparison between the clinical-based and MRI-based NCCN classification: 50 (21.7%) patients were upgraded to a higher risk group after mpMRI, 169 (73.4%) remained in the same MRI-based NCCN risk group as their clinical NCCN risk group and 11 (4.7%) were downgraded to a lower risk group.

Thus, 85 (36.9%) patients were classified as low risk according to MRI-based NCCN, 82 (35.6%) patients in the intermediate group, 50 (21.7%) in high risk and 13 (5.6%) in the very high risk group.

Univariate and multivariate analyses of predictors of biochemical relapse

The median follow-up time since the date of diagnostic was 8.7 years (IQR, 6.6–10.1) and the biochemical relapse-free survival rate was 88.4% (95% CI: 83.4–92.0%) at 5 years and 62.9% (95% CI: 53.7–70.8%) at 10 years (*Figure 3*).

A summary of the univariate analysis is available in *Table 3* and the different models used in the multivariate analysis are summarized in *Table 4* and *Table 5*.

All of these models have made it possible to highlight certain independent factors of biochemical relapse: the MRI-based NCCN classification, the ECE and the Cho/Cit ratio in healthy tissue in TZ.

Discussion

The present study showed that, among patients with newly diagnosed localized prostate cancer, mpMRI combined with proton spectroscopy, could aid in prognostic stratification following radiotherapy.

We have identified 3 independent predictors of biochemical relapse in this population: high-risk MRI-based NCCN classification, presence of an ECE on mpMRI, and a high Cho/Cit ratio in healthy TZ tissue.

These results suggest the hypothesis that the T-MRI classification is more efficient than the T-clinical classification to predict patient outcomes, the traditional NCCN classification not appearing as an independent factor of recurrence in our analysis.

Most studies to date have focused on the prognostic value of mpMRI at diagnosis in studies where the T-stage and Gleason score were established on prostatectomy specimens (35,36). This gold standard of tumor T-stage cannot be used in studies focused on non-surgical therapies such as radiotherapy where the T-stage is still established on the Gleason grade of biopsies and the digital rectal examination.

Our results lead us to consider MRI T-stage, and therefore the MRI-based NCCN classification, as an essential prognostic factor in these situations.

ECE is a recognized prognostic factor (37) reflecting a more aggressive disease, classifying it at least as a T3 stage, with an increased risk of metastatic spread as demonstrated in the study of McKenna *et al.* (38) where ECE was, with a threshold of 5 mm, the only independent factor for occurrence of metastatic relapse.

On the other hand, Yu *et al.* (20) have demonstrated in a retrospective study that the combination of mpMRI and spectroscopic analyses reduced inter-observer variability in the diagnosis of ECE on pre-therapeutic mpMRI, using the ratio choline/citrate >2SD to detect tumor boundaries.

In our study, only high Cho/Cit ratio in healthy tissue in TZ returned as an independent factor of biochemical relapse in all three models tested, with quite comparative HR. Indeed, if we decompose this ratio by the

© Quantitative Imaging in Medicine and Surgery. All rights reserved.

Table 2 mpMRI parameters according to absence or presence of biochemical relapse

Variables	Entire cohort	No biochemical relapse	Biochemical relapse	P value
N	230	193	37	
Prostatic volume (mL)	46.7 [37.5–62.5]	46.2 [37.5–62.5]	52.9 [38.3–61.3]	0.8
Number of lesions				
0	29	28 (14.5)	1 (2.7)	0.03
1	187	156 (80.8)	31 (83.8)	
2	15	10 (5.2)	5 (13.5)	
Tumor location				
PZ	191 (88.4)	146 (88.0)	34 (94.4)	0.5
TZ	24 (11.1)	19 (11.4)	2 (5.6)	
AFS	1 (0.5)	1 (0.6)	0 (0.0)	
Tumor size (mm)	15.5 [11.0–21.0]	15 [11.0–20.0]	20 [14.5–28.0]	<0.01
Seminal vesicles extension	9 (4.0)	6 (3.6)	3 (8.3)	0.2
Capsular contact	168 (83.2)	137 (82.5)	31 (86.1)	0.6
Contact capsular length (mm)	11.0 [7.0–19.5]	10.0 [7.0–17.0]	19.0 [10.0–27.0]	<0.01
Extracapsular extension	55 (27.2)	33 (19.9)	22 (61.1)	<0.01
Extension thickness (mm)	4.0 [3.0–5.0]	3.0 [3.0–4.0]	4.0 [4.0–6.0]	<0.01
Tumor ADC (mm^2/s)	842 [667.0–1,056.0]	852.0 [683.0–1,089.0]	717.0 [598.0–986.5]	0.04
Tumor DWI size (mm)	14.0 [10.0–19.0]	13.0 [10.0–18.0]	18.0 [13.0–21.0]	<0.01
Wash-in coefficient	224.5 [179.0–267.0]	223.0 [170.0–264.0]	237.5 [209.5–287.5]	0.04
Average of the lowest 10% of ADC (mm^2/s)	501.0 [341.0–696.0]	512.0 [366.0–702.0]	429.5 [237.0–673.5]	0.07
PI-RADS v2.1				
1–2	28 (12.1)	27 (13.9%)	1 (2.7%)	<0.01
3	26 (11.3)	26 (13.5%)	0 (0.0%)	
4	70 (30.4)	63 (32.6%)	7 (18.9%)	
5	106 (46.1)	77 (39.9%)	29 (78.4%)	
MRI T-stage				
T1c	29 (12.6)	28 (14.5)	1 (2.7)	<0.01
T2a	98 (42.6)	91 (47.2)	7 (18.9)	
T2b	38 (16.5)	33 (17.1)	5 (13.5)	
T2c	12 (5.2)	10 (5.2)	2 (5.4)	
T3a	44 (19.1)	25 (13.0)	19 (51.4)	
T3b	9 (3.9)	6 (3.1)	3 (8.1)	
MRI-based NCCN risk group				
Low	85 (37.0)	81 (42.0)	4 (10.8)	<0.01
Intermediate	82 (35.7)	72 (37.3)	10 (27.0)	
High	50 (21.7)	32 (16.6)	18 (48.6)	
Very high	13 (5.7)	8 (4.1)	5 (13.5)	

All values are median [Q1–Q3] or number (percentage). mpMRI, multiparametric magnetic resonance imaging; PZ, peripheral zone; TZ, transition zone; AFS, anterior fibromuscular stroma; ADC, apparent diffusion coefficient; DWI, diffusion weighted images; PI-RADS v2.1, Prostate Imaging Reporting and Data System version 2.1; MRI, magnetic resonance imaging; NCCN, National Comprehensive Cancer Network.

© Quantitative Imaging in Medicine and Surgery. All rights reserved.

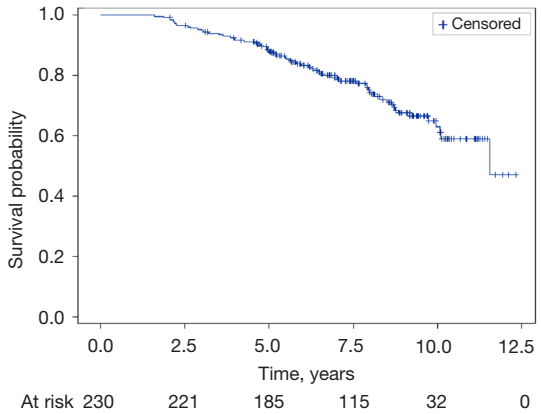

Figure 3 Biochemical relapse-free survival.

concentrations of each metabolite, we note that the risk of recurrence is only related to early variations in citrate, the latter being a protective factor in all multivariate models if its pool is >7 mmol/L in healthy tissue in TZ.

Choline and citrate are two important metabolites in prostate function but also in tumor tissue. Citrate is a crucial element in prostate energy metabolism, whose levels vary more significantly than those of choline, which rather reflects the degree of tumor membrane cell activity. The early decrease in citrate is therefore due to both changes in cellular function and in the organization of the tissue, but may also decrease in prostatitis, when the choline level increases proportionally to tumor cell proliferation or in the

Table 3 Predictors of biochemical relapse by univariate Cox analysis

Variables	HR	95% CI	P value
Clinical T-stage, N=230			
T2 *vs.* T1c	1.811	1.055–3.110	0.03
T3 *vs.* T1c	2.359	1.120–4.965	
PSA max pre-treatment, N=230			
>7.5 *vs.* ≤7.5 ng/mL	2.205	1.306–3.725	<0.01
Gleason, N=230			
≥4+3 *vs.* ≤3+4	2.014	1.094–3.706	0.02
7–10 *vs.* 4–6	2.256	1.38–3.689	<0.01
Clinical-based D'Amico risk group, N=230			
High *vs.* low	3.01	1.586–5.711	<0.01
Intermediate *vs.* low	2.171	1.159–4.069	
Clinical-based NCCN risk group, N=230			
High & very high *vs.* low	2.634	1.282–5.410	<0.01
Intermediate *vs.* low	2.454	1.354–4.448	
MRI-based D'Amico risk group, N=230			
High *vs.* low	5.583	2.692–11.576	<0.01
Intermediate *vs.* low	2.465	1.107–5.490	
MRI-based NCCN risk group, N=230			
High *vs.* low	5.803	2.735–12.312	<0.01
Intermediate *vs.* low	2.477	1.127–5.442	
Very high *vs.* low	6.797	2.526–18.288	
Wash in coefficient TZ, N=230			
>170 *vs.* ≤170	0.462	0.271-0.787	<0.01

Table 3 (*continued*)

© Quantitative Imaging in Medicine and Surgery. All rights reserved.

Table 3 (*continued*)

Variables	HR	95% CI	P value
Tumor size, N=230			
>15 *vs.* ≤15 mm	2.460	1.415–4.279	<0.01
Extracapsular extension, N=230			
Yes *vs.* no	3.672	2.206–6.110	<0.01
Tumor ADC, N=230			
>640 *vs.* ≤640 mm^2/s	0.538	0.313–0.922	0.02
Tumor DWI size, N=230			
≥14 *vs.* <14 mm	2.562	1.502–4.370	<0.01
MRI T-stage, N=230			
T2 *vs.* T1c	1.509	0.529–4.305	<0.01
T3 *vs.* T1c	5.161	1.823–14.609	
PI-RADS v2.1, N=230			
4–5 *vs.* 1–3	3.372	1.454–7.820	<0.01
Citrate tumor PZ, N=171			
>2 *vs.* ≤2	0.424	0.180–1.003	0.05
Citrate healthy tissue PZ, N=208			
>9.6 *vs.* ≤9.6	0.526	0.265–1.041	0.06
Citrate healthy tissue TZ, N=207			
>7 *vs.* ≤7	0.506	0.255–1.004	0.05
Choline tumor PZ, N=171			
>3.3 *vs.* ≤3.3	1.756	1.001–3.081	0.04
Choline healthy tissue PZ, N=208			
>3.3 *vs.* ≤3.3	2.851	1.475–5.511	<0.01
Choline healthy tissue TZ, N=207			
>1.5 *vs.* ≤1.5	2.866	0.896–9.164	0.07
Choline/Citrate tumor PZ, N=171			
>0.15 *vs.* ≤0.15	2.061	0.879–4.832	0.09
Choline/Citrate healthy tissue PZ, N=208			
>0.25 *vs.* ≤0.25	2.092	1.082–4.043	0.03
Choline/Citrate healthy tissue TZ, N=207			
>0.1 *vs.* ≤0.1	2.972	1.186–7.450	0.02

HR, hazard ratio; CI, confidence interval; PSA, prostate specific antigen; NCCN, National Comprehensive Cancer Network; MRI, magnetic resonance imaging; TZ, transition zone; ADC, apparent diffusion coefficient; DWI, diffusion weighted images; PI-RADS v2.1, Prostate Imaging Reporting and Data System version 2.1; PZ, peripheral zone.

© Quantitative Imaging in Medicine and Surgery. All rights reserved.

Table 4 Predictors of biochemical relapse by multivariate Cox analysis using the Choline/Citrate ratio

Variables	HR	95% CI	P value	Harrell C
Model 1 using MRI-based NCCN risk group, N=181				
Choline/Citrate healthy tissue TZ			0.04	
>0.1 *vs.* ≤0.1	2.969	1.064–8.286		
MRI-based NCCN risk group			<0.01	0.72
Intermediate risk *vs.* low risk	3.067	1.133–8.306		
High & very high risk *vs.* low risk	7.003	2.711–18.091		
Wash in coefficient TZ			0.03	
>170 *vs.* ≤170	0.513	0.276–0.955		
Model 2 using extracapsular extension, N=182				
Choline/Citrate healthy tissue TZ			0.04	
>0.1 *vs.* ≤0.1	2.857	1.024–7.970		0.7
Extracapsular extension			<0.01	
Yes *vs.* no	3.332	1.936–5.736		
Wash in coefficient TZ			0.04	
>170 *vs.* ≤170	0.517	0.277–0.966		
Model 3 using PI-RADS v2.1, N=181				
Choline/Citrate healthy tissue TZ			0.03	
>0.1 *vs.* ≤0.1	3.029	1.092–8.404		
PI-RADS v2.1			0.05	
4–5 *vs.* 1–3	7.123	0.982–51.642		0.67
Wash in coefficient TZ			0.01	
>170 *vs.* ≤170	0.447	0.241–0.828		
Average of the lowest 10% of ADC			0.02	
>270 *vs.* ≤270 mm^2/s	0.481	0.264–0.878		

HR, hazard ratio; CI, confidence interval; MRI, magnetic resonance imaging; NCCN, National Comprehensive Cancer Network; TZ, transition zone; PI-RADS v2.1, Prostate Imaging Reporting and Data System version 2.1; ADC, apparent diffusion coefficient.

case of necrosis, a phenomenon which is mainly visible in undifferentiated tumors, particularly with a high Gleason grade (39). Indeed, the use of metabolite concentrations may even be more pertinent than simple ratios, commonly used in the literature, as shown in the recent study by Deal *et al.* (40) in which spectroscopic data showed that the choline concentration was significantly higher in aggressive disease. Moreover, in their study, the predictive model of tumor aggressiveness combining mpMRI and 3D MRS was better than the mpMRI model alone.

Biochemically, high concentrations of citrate are maintained because there is a permanent inhibition of its oxidation in the Krebs cycle thanks to levels of zinc which will prevent the enzymatic activity of m-aconitase from reducing the citrate to isocitrate (41). Thus, it has been proven that early and even at low Gleason (ex. 3+3), there is not an increase in the production of m-aconitase but in its activity secondary to the decrease in intraprostatic zinc content due to the alteration of an essential transporter, ZIP1 (42). Thus, the joint study of citrate levels in spectroscopy and zinc in biochemistry could be an early marker of tumor invasion, well before having histological

© Quantitative Imaging in Medicine and Surgery. All rights reserved.

Table 5 Predictors of biochemical relapse by multivariate Cox analysis using Choline and Citrate concentrations

Variables	HR	95% CI	P value	Harrell C
Model 1 using MRI-based NCCN risk group, N=181				
Citrate healthy tissue TZ			0.01	
>7 *vs.* ≤7 mmol/L	0.41	0.201–0.837		
MRI-based NCCN risk group			<0.01	0.73
Intermediate risk *vs*. low risk	2.967	1.089–8.086		
High & very high risk *vs.* low risk	6.617	2.538–17.255		
Wash in coefficient TZ			0.03	
>170 *vs.* ≤170	0.574	0.275–0.955		
Model 2 using extracapsular extension, N=182				
Choline healthy tissue TZ			0.4	
>1.5 *vs.* ≤1.5 mmol/L	1.574	0.480–5.165		
Citrate healthy tissue TZ			0.03	
>7 *vs.* ≤7 mmol/L	0.453	0.225–0.913		0.7
Extracapsular extension			<0.01	
Yes *vs.* no	3.369	1.948–5.825		
Wash in coefficient TZ			0.04	
>170 *vs.* ≤170	0.52	0.277–0.975		
Model 3 using PI-RADS v2.1, N=181				
Citrate healthy tissue TZ			0.04	
>7 *vs.* ≤7 mmol/L	0.487	0.241–0.986		
PI-RADS v2.1			0.07	
4–5 *vs.* 1–3	6.239	0.858–45.386		0.66
Wash in coefficient TZ			0.01	
>170 *vs.* ≤170	0.439	0.235–0.819		
Average of the lowest 10% of ADC			0.01	
>270 *vs.* ≤270 mm^2/s	0.466	0.253–0.861		

HR, hazard ratio; CI, confidence interval; MRI, magnetic resonance imaging; NCCN, National Comprehensive Cancer Network; TZ, transition zone; PI-RADS v2.1, Prostate Imaging Reporting and Data System version 2.1; ADC, apparent diffusion coefficient.

proof (43).

Moreover, as the PZ is basically richer in citrate due to its glandular nature, it seems logical to demonstrate in our study a significant difference in the fall of citrate in TZ earlier than in PZ.

Casciani *et al.* (44) showed that normal concentrations of citrate in the PZ were only found in cases of well-differentiated tumors, with a low Gleason grade, a significant drop in citrate being a marker of tumor dedifferentiation. This is in accordance with our population who relapsed, composed mainly of low Gleason grade: 45.9% of Gleason 6 and 40.5% of Gleason 7 (29.7% of 3+4).

Thus, spectroscopic analysis can be a useful tool to assess tumor differentiation and biological aggressiveness.

It has been known for a decade that the performance of prostate cancer detection with mpMRI is dependent on tumor volume and the Gleason histological score. Our mpMRI tumor detection rate was 88.5%, in accordance

© Quantitative Imaging in Medicine and Surgery. All rights reserved.

with the data in the literature after Styles *et al.* (45) that demonstrated a sensitivity of 85% for the detection of lesions greater than 0.5 cc at 3T MRI. Moreover, a systematic review of 66 studies in 2017 (46) reported detection of index lesions in 90% of cases. This is clearly supported by our results because mpMRI could detect a significant lesion in 78% of patients considered as clinical T1c, i.e. in whom the digital rectal examination was not pathological, and thus reclassified them in a higher risk group.

More generally, we noted that 152 patients did not have the same concordance between their initial clinical T-stage and their MRI T-stage, and particularly 128 patients had higher MRI T-stage, i.e., a final reclassification of 21.7% of patients into a higher-risk group according to the NCCN-MRI classification. These results are consistent with those of Gomez-Iturriaga *et al.* (47) who demonstrated that 38% of patients initially considered T1 or T2 were reclassified T3 MRI and therefore 35% reclassified as high risk after mpMRI analyses. These results are also suggested in the retrospective study by Couñago *et al.* (48) published in 2015 where 16.7% of the 269 patients initially classified as clinical T1 or T2 were reclassified after mpMRI analysis as T3 or T4.

It is therefore recognized that mpMRI has a decisive role in the re-evaluation of the tumor T-stage, and also modifies the prognostic classification of patients by improving the detection of lesions and their characterization (49).

The initial demographical characteristics of our patients were conforming to data in the literature: the average age at diagnosis (67.5 years) was comparable to the average age (70 years) in French cancers registries in 2011.

Our study population represented the heterogeneity of localized prostate cancers, with 51.7% of T1c clinical T-stage, 14.8% of T2a and 9.6% of T2c for example, with histopathological diagnosis of 65.2% of Gleason 6, 30.4% of Gleason 7 and 3% of Gleason 8 and more.

Thus, we had a large proportion of low (43.0%) and intermediate risk (42.2%) patients according to NCCN-clinical classification.

The median duration of our follow-up was long [8.7 years (IQR, 6.6–10.1 years)] compared with many studies where it varies regularly between 36 months and 6 years (50-53), thus reinforcing the credibility of our concluding observations regarding long term survival in our study.

Survival data at 5 years (88.4%) and 10 years (62.9%) are less favorable than those reported by the French National Institut of CAncer (INCA) in 2021, i.e., 93% at 5 years and 80% at 10 years. This difference might be explained by the improvement of tumor detection techniques, staging and management over the last 10 years.

The biochemical relapse rate of prostate cancer after EBRT or BT in our population (16%) was similar to the results of the study conducted by Lazarev *et al.* in 2018, estimated at 13.9% (54).

Thus, our study population was wholly representative of French prostate localized cancers, particularly those of low and intermediate risk according to the NCCN-clinical classification.

The major strengths of our study rely on the homogeneity of mpMRI acquisition protocol and on the interpretation of images by an experienced team as well as the protocolised treatments delivered in an academic center specialized in cancers treatments. However, our study also has some limitations. First, it is a single institution retrospective study and our results would need to be confirmed by a global study integrating more centers. Moreover, it will be interesting to include more patients classified as high risk according to the NCCN-clinical classification, with an increased risk of metastasis and worse prognostic, and to carry out on a more homogeneous population a study concerning the patients treated by several treatments, those being able to interfere in the biochemical relapse-free. Therefore, the fact of initially choosing in the inclusion criteria two different treatments may also be at the origin of confounding biases, although it does reflect all the heterogeneity of the management of our patients, and thus the reality of daily situations. The choice of the date of diagnosis as a benchmark for the follow-up of biochemical recurrence-free survival may have led in our study to an immortal time bias, despite a low median latency between diagnosis and end of treatment (5.1 months). One of the major strengths of our study i.e., the use of the same mpMRI acquisition protocol throughout the study could also be considered as a limitation. Indeed, at the onset of the study in 2008, high b-value DWI was not routine and image quality at 3T was not optimal. We stood by our choice of using an unchanged protocol until 2015, where an upgrade allowed high b-value DWI.

We noted that the wash-in variable in the TZ emerged significantly with almost the same risk in the 3 models (HR =0.5) as a protective factor of biochemical relapse. We were not able to explain this result with respect to the literature. It seems difficult to interpret the value of this isolated parameter without a parallel wash-out study.

© Quantitative Imaging in Medicine and Surgery. All rights reserved.

Conclusions

In conclusion, the quantitative analysis of prostate metabolism with 3D MRS combined with morphologic and functional analyses in our retrospective study has shown a great potential for prognostic stratification in patients with localized prostate tumors treated by EBRT or BT. We were able to define 3 independent predictive factors of biochemical relapse, which are the MRI-based NCCN risk classification, the Cho/Cit ratio in healthy tissue in TZ and presence of ECE. These results emphasize the potential interest of advanced quantification of the target lesion but also of the "healthy" prostate gland, beyond simple estimation of PI-RADS score, for prognostic stratification and then potentially for orientation of therapeutic and follow-up strategies. A prognostic classification including mpMRI analysis and 3D MRS could be more appropriate for treatment guidance.

It would be worthwhile to propose a multicenter study with a larger population to reinforce the link between these different elements or a secondary study looking at intra prostatic zinc levels to support our spectroscopic data.

Acknowledgments

Funding: None.

Footnote

Reporting Checklist: The authors have completed the STROBE reporting checklist. Available at https://qims.amegroups.com/article/view/10.21037/qims-22-184/rc

Conflicts of Interest: All authors have completed the ICMJE uniform disclosure form (available at https://qims.amegroups.com/article/view/10.21037/qims-22-184/coif). RL serves as an unpaid Deputy Editor of *Quantitative Imaging in Medicine and Surgery*. AC serves as an unpaid editorial board member of *Quantitative Imaging in Medicine and Surgery*. The other authors have no conflicts of interest to declare.

Ethical Statement: The authors are accountable for all aspects of the work in ensuring that questions related to the accuracy or integrity of any part of the work are appropriately investigated and resolved. The study was conducted in accordance with the Declaration of Helsinki (as revised in 2013). The study was approved by the ethics committee of the University Hospital of Dijon and individual consent for this retrospective analysis was waived.

Open Access Statement: This is an Open Access article distributed in accordance with the Creative Commons Attribution-NonCommercial-NoDerivs 4.0 International License (CC BY-NC-ND 4.0), which permits the non-commercial replication and distribution of the article with the strict proviso that no changes or edits are made and the original work is properly cited (including links to both the formal publication through the relevant DOI and the license). See: https://creativecommons.org/licenses/by-nc-nd/4.0/.

References

1. D'Amico AV, Whittington R, Malkowicz SB, Schultz D, Blank K, Broderick GA, Tomaszewski JE, Renshaw AA, Kaplan I, Beard CJ, Wein A. Biochemical outcome after radical prostatectomy, external beam radiation therapy, or interstitial radiation therapy for clinically localized prostate cancer. JAMA 1998;280:969-74.
2. Mohler JL, Antonarakis ES, Armstrong AJ, D'Amico AV, Davis BJ, Dorff T, et al. Prostate Cancer, Version 2.2019, NCCN Clinical Practice Guidelines in Oncology. J Natl Compr Canc Netw 2019;17:479-505.
3. Neppl-Huber C, Zappa M, Coebergh JW, Rapiti E, Rachtan J, Holleczek B, Rosso S, Aareleid T, Brenner H, Gondos A; EUNICE Survival Working Group. Changes in incidence, survival and mortality of prostate cancer in Europe and the United States in the PSA era: additional diagnoses and avoided deaths. Ann Oncol 2012;23:1325-34.
4. Agarwal PK, Sadetsky N, Konety BR, Resnick MI, Carroll PR; Cancer of the Prostate Strategic Urological Research Endeavor (CaPSURE). Treatment failure after primary and salvage therapy for prostate cancer: likelihood, patterns of care, and outcomes. Cancer 2008;112:307-14.
5. Wang N, Gerling GJ, Childress RM, Martin ML. Quantifying palpation techniques in relation to performance in a clinical prostate exam. IEEE Trans Inf Technol Biomed 2010;14:1088-97.
6. Naji L, Randhawa H, Sohani Z, Dennis B, Lautenbach D, Kavanagh O, Bawor M, Banfield L, Profetto J. Digital Rectal Examination for Prostate Cancer Screening in Primary Care: A Systematic Review and Meta-Analysis. Ann Fam Med 2018;16:149-54.
7. Beyersdorff D, Taupitz M, Winkelmann B, Fischer T, Lenk S, Loening SA, Hamm B. Patients with a history of elevated prostate-specific antigen levels and negative

© Quantitative Imaging in Medicine and Surgery. All rights reserved.

transrectal US-guided quadrant or sextant biopsy results: value of MR imaging. Radiology 2002;224:701-6.
8. Rouvière O, Puech P, Renard-Penna R, Claudon M, Roy C, Mège-Lechevallier F, Decaussin-Petrucci M, Dubreuil-Chambardel M, Magaud L, Remontet L, Ruffion A, Colombel M, Crouzet S, Schott AM, Lemaitre L, Rabilloud M, Grenier N; MRI-FIRST Investigators. Use of prostate systematic and targeted biopsy on the basis of multiparametric MRI in biopsy-naive patients (MRI-FIRST): a prospective, multicentre, paired diagnostic study. Lancet Oncol 2019;20:100-9.
9. Dickinson L, Ahmed HU, Allen C, Barentsz JO, Carey B, Futterer JJ, Heijmink SW, Hoskin PJ, Kirkham A, Padhani AR, Persad R, Puech P, Punwani S, Sohaib AS, Tombal B, Villers A, van der Meulen J, Emberton M. Magnetic resonance imaging for the detection, localisation, and characterisation of prostate cancer: recommendations from a European consensus meeting. Eur Urol 2011;59:477-94.
10. Harvey H, deSouza NM. The role of imaging in the diagnosis of primary prostate cancer. J Clin Urol 2016;9:11-7.
11. Aydin H, Kizilgöz V, Tatar IG, Damar C, Ugan AR, Paker I, Hekimoğlu B. Detection of prostate cancer with magnetic resonance imaging: optimization of T1-weighted, T2-weighted, dynamic-enhanced T1-weighted, diffusion-weighted imaging apparent diffusion coefficient mapping sequences and MR spectroscopy, correlated with biopsy and histopathological findings. J Comput Assist Tomogr 2012;36:30-45.
12. Claus FG, Hricak H, Hattery RR. Pretreatment evaluation of prostate cancer: role of MR imaging and 1H MR spectroscopy. Radiographics 2004;24 Suppl 1:S167-80.
13. Wang L, Mullerad M, Chen HN, Eberhardt SC, Kattan MW, Scardino PT, Hricak H. Prostate cancer: incremental value of endorectal MR imaging findings for prediction of extracapsular extension. Radiology 2004;232:133-9.
14. Turkbey B, Rosenkrantz AB, Haider MA, Padhani AR, Villeirs G, Macura KJ, Tempany CM, Choyke PL, Cornud F, Margolis DJ, Thoeny HC, Verma S, Barentsz J, Weinreb JC. Prostate Imaging Reporting and Data System Version 2.1: 2019 Update of Prostate Imaging Reporting and Data System Version 2. Eur Urol 2019;76:340-51.
15. Rajwa P, Mori K, Huebner NA, Martin DT, Sprenkle PC, Weinreb JC, Ploussard G, Pradere B, Shariat SF, Leapman MS. The Prognostic Association of Prostate MRI PI-RADS™ v2 Assessment Category and Risk of Biochemical Recurrence after Definitive Local Therapy for Prostate Cancer: A Systematic Review and Meta-Analysis. J Urol 2021;206:507-16.
16. Pockros B, Stensland KD, Parries M, Frankenberger E, Canes D, Moinzadeh A. Preoperative MRI PI-RADS scores are associated with prostate cancer upstaging on surgical pathology. Prostate 2022;82:352-8.
17. Chitkara M, Westphalen A, Kurhanewicz J, Qayyum A, Poder L, Reed G, Coakley FV. Magnetic resonance spectroscopic imaging of benign prostatic tissue: findings at 3.0 T compared to 1.5 T-initial experience. Clin Imaging 2011;35:288-93.
18. Gholizadeh N, Greer PB, Simpson J, Goodwin J, Fu C, Lau P, Siddique S, Heerschap A, Ramadan S. Diagnosis of transition zone prostate cancer by multiparametric MRI: added value of MR spectroscopic imaging with sLASER volume selection. J Biomed Sci 2021;28:54.
19. Scheidler J, Hricak H, Vigneron DB, Yu KK, Sokolov DL, Huang LR, Zaloudek CJ, Nelson SJ, Carroll PR, Kurhanewicz J. Prostate cancer: localization with three-dimensional proton MR spectroscopic imaging--clinicopathologic study. Radiology 1999;213:473-80.
20. Yu KK, Scheidler J, Hricak H, Vigneron DB, Zaloudek CJ, Males RG, Nelson SJ, Carroll PR, Kurhanewicz J. Prostate cancer: prediction of extracapsular extension with endorectal MR imaging and three-dimensional proton MR spectroscopic imaging. Radiology 1999;213:481-8.
21. Zackrisson B, Aus G, Bergdahl S, Lilja H, Lodding P, Pihl CG, Hugosson J. The risk of finding focal cancer (less than 3 mm) remains high on re-biopsy of patients with persistently increased prostate specific antigen but the clinical significance is questionable. J Urol 2004;171:1500-3.
22. Coakley FV, Teh HS, Qayyum A, Swanson MG, Lu Y, Roach M 3rd, Pickett B, Shinohara K, Vigneron DB, Kurhanewicz J. Endorectal MR imaging and MR spectroscopic imaging for locally recurrent prostate cancer after external beam radiation therapy: preliminary experience. Radiology 2004;233:441-8.
23. Westphalen AC, Coakley FV, Roach M 3rd, McCulloch CE, Kurhanewicz J. Locally recurrent prostate cancer after external beam radiation therapy: diagnostic performance of 1.5-T endorectal MR imaging and MR spectroscopic imaging for detection. Radiology 2010;256:485-92.
24. Westphalen AC, Coakley FV, Qayyum A, Swanson M, Simko JP, Lu Y, Zhao S, Carroll PR, Yeh BM, Kurhanewicz J. Peripheral zone prostate cancer: accuracy of different interpretative approaches with MR and MR spectroscopic imaging. Radiology 2008;246:177-84.
25. Cuschieri S. The STROBE guidelines. Saudi J Anaesth

© Quantitative Imaging in Medicine and Surgery. All rights reserved.

2019;13:S31-4.
26. Kandori S, Kojima T, Nishiyama H. The updated points of TNM classification of urological cancers in the 8th edition of AJCC and UICC. Jpn J Clin Oncol 2019;49:421-5.
27. Rozet F, Hennequin C, Beauval JB, et al. French ccAFU guidelines - Update 2018-2020: Prostate cancer. Prog Urol 2018 Nov;28 Suppl 1:R81-R132.
28. Roach M 3rd, Hanks G, Thames H Jr, Schellhammer P, Shipley WU, Sokol GH, Sandler H. Defining biochemical failure following radiotherapy with or without hormonal therapy in men with clinically localized prostate cancer: recommendations of the RTOG-ASTRO Phoenix Consensus Conference. Int J Radiat Oncol Biol Phys 2006;65:965-74.
29. Scheenen TW, Heijmink SW, Roell SA, Hulsbergen-Van de Kaa CA, Knipscheer BC, Witjes JA, Barentsz JO, Heerschap A. Three-dimensional proton MR spectroscopy of human prostate at 3 T without endorectal coil: feasibility. Radiology 2007;245:507-16.
30. Barentsz JO, Richenberg J, Clements R, Choyke P, Verma S, Villeirs G, Rouviere O, Logager V, Fütterer JJ; European Society of Urogenital Radiology. ESUR prostate MR guidelines 2012. Eur Radiol 2012;22:746-57.
31. Weinreb JC, Barentsz JO, Choyke PL, Cornud F, Haider MA, Macura KJ, Margolis D, Schnall MD, Shtern F, Tempany CM, Thoeny HC, Verma S. PI-RADS Prostate Imaging - Reporting and Data System: 2015, Version 2. Eur Urol 2016;69:16-40.
32. Giganti F, Allen C. Imaging quality and prostate MR: it is time to improve. Br J Radiol 2021;94:20200934.
33. Lee CH, Taupitz M, Asbach P, Lenk J, Haas M. Clinical utility of combined T2-weighted imaging and T2-mapping in the detection of prostate cancer: a multi-observer study. Quant Imaging Med Surg 2020;10:1811-22.
34. Park H, Kim SH, Kim JY. Dynamic contrast-enhanced magnetic resonance imaging for risk stratification in patients with prostate cancer. Quant Imaging Med Surg 2022;12:742-51.
35. Park BH, Jeon HG, Jeong BC, Seo SI, Lee HM, Choi HY, Jeon SS. Influence of magnetic resonance imaging in the decision to preserve or resect neurovascular bundles at robotic assisted laparoscopic radical prostatectomy. J Urol 2014;192:82-8.
36. Cheng L, Slezak J, Bergstralh EJ, Myers RP, Zincke H, Bostwick DG. Preoperative prediction of surgical margin status in patients with prostate cancer treated by radical prostatectomy. J Clin Oncol 2000;18:2862-8.
37. Riaz N, Afaq A, Akin O, Pei X, Kollmeier MA, Cox B, Hricak H, Zelefsky MJ. Pretreatment endorectal coil magnetic resonance imaging findings predict biochemical tumor control in prostate cancer patients treated with combination brachytherapy and external-beam radiotherapy. Int J Radiat Oncol Biol Phys 2012;84:707-11.
38. McKenna DA, Coakley FV, Westphalen AC, Zhao S, Lu Y, Webb EM, Pickett B, Roach M 3rd, Kurhanewicz J. Prostate cancer: role of pretreatment MR in predicting outcome after external-beam radiation therapy--initial experience. Radiology 2008;247:141-6.
39. Wang XZ, Wang B, Gao ZQ, Liu JG, Liu ZQ, Niu QL, Sun ZK, Yuan YX. 1H-MRSI of prostate cancer: the relationship between metabolite ratio and tumor proliferation. Eur J Radiol 2010;73:345-51.
40. Deal M, Bardet F, Walker PM, de la Vega MF, Cochet A, Cormier L, Bentellis I, Loffroy R. Three-dimensional nuclear magnetic resonance spectroscopy: a complementary tool to multiparametric magnetic resonance imaging in the identification of aggressive prostate cancer at 3.0T. Quant Imaging Med Surg 2021;11:3749-66.
41. Costello LC, Franklin RB. Citrate metabolism of normal and malignant prostate epithelial cells. Urology 1997;50:3-12.
42. Singh KK, Desouki MM, Franklin RB, Costello LC. Mitochondrial aconitase and citrate metabolism in malignant and nonmalignant human prostate tissues. Mol Cancer 2006;5:14.
43. Costello LC, Liu Y, Franklin RB, Kennedy MC. Zinc inhibition of mitochondrial aconitase and its importance in citrate metabolism of prostate epithelial cells. J Biol Chem 1997;272:28875-81.
44. Casciani E, Polettini E, Bertini L, Emiliozzi P, Amini M, Pansadoro V, Gualdi GF. Prostate cancer: evaluation with endorectal MR imaging and three-dimensional proton MR spectroscopic imaging. Radiol Med 2004;108:530-41.
45. Styles C, Ferris N, Mitchell C, Murphy D, Frydenberg M, Mills J, Pedersen J, Bergen N, Duchesne G. Multiparametric 3T MRI in the evaluation of intraglandular prostate cancer: correlation with histopathology. J Med Imaging Radiat Oncol 2014;58:439-48.
46. Monni F, Fontanella P, Grasso A, Wiklund P, Ou YC, Randazzo M, Rocco B, Montanari E, Bianchi G. Magnetic resonance imaging in prostate cancer detection and management: a systematic review. Minerva Urol Nefrol 2017;69:567-78.

© Quantitative Imaging in Medicine and Surgery. All rights reserved.

47. Gomez-Iturriaga A, Casquero F, Pijoan JI, Crook J, Urresola A, Ezquerro A, Villeirs GM, Bossi A, Cacicedo J, Buchser D, Bilbao P. Pretreatment Multiparametric Magnetic Resonance Imaging Findings Are More Accurate Independent Predictors of Outcome Than Clinical Variables in Localized Prostate Cancer. Int J Radiat Oncol Biol Phys 2018;101:1172-8.
48. Couñago F, Del Cerro E, Díaz-Gavela AA, Marcos FJ, Recio M, Sanz-Rosa D, Thuissard I, Olaciregui K, Mateo M, Cerezo L. Tumor staging using 3.0 T multiparametric MRI in prostate cancer: impact on treatment decisions for radical radiotherapy. Springerplus 2015;4:789.
49. Krausewitz P, Ritter M. Clinical aspects in the diagnosis and treatment of prostate cancer. Radiologe 2021;61:795-801.
50. Delouya G, Krishnan V, Bahary JP, et al. Analysis of the Cancer of the Prostate Risk Assessment to predict for biochemical failure after external beam radiotherapy or prostate seed brachytherapy. Urology 2014;84:629-33.
51. Delouya G, Lambert C, Bahary JP, Beauchemin MC, Barkati M, Ménard C, Taussky D. Comparison of external beam radiotherapy versus permanent seed brachytherapy as monotherapy for intermediate-risk prostate cancer - a single center Canadian experience. Can J Urol 2017;24:8822-6.
52. Krishnan V, Delouya G, Bahary JP, Larrivée S, Taussky D. The Cancer of the Prostate Risk Assessment (CAPRA) score predicts biochemical recurrence in intermediate-risk prostate cancer treated with external beam radiotherapy (EBRT) dose escalation or low-dose rate (LDR) brachytherapy. BJU Int 2014;114:865-71.
53. Yoshida K, Yamazaki H, Nakamura S, Masui K, Kotsuma T, Akiyama H, Tanaka E, Yoshioka Y. Role of novel risk classification method, Prostate Cancer Risk Index (PRIX) for clinically localized prostate cancer after high-dose-rate interstitial brachytherapy as monotherapy. Anticancer Res 2014;34:3077-81.
54. Lazarev S, Thompson MR, Stone NN, Stock RG. Low-dose-rate brachytherapy for prostate cancer: outcomes at >10 years of follow-up. BJU Int 2018;121:781-90.

Cite this article as: Asuncion A, Walker PM, Bertaut A, Blanc J, Labarre M, Martin E, Bardet F, Cassin J, Cormier L, Crehange G, Loffroy R, Cochet A. Prediction of prostate cancer recurrence after radiation therapy using multiparametric magnetic resonance imaging and spectroscopy: assessment of prognostic factors on pretreatment imaging. Quant Imaging Med Surg 2022;12(12):5309-5325. doi: 10.21037/qims-22-184

© Quantitative Imaging in Medicine and Surgery. All rights reserved.

Supplementary

Table S1 Spectroscopic analyses

Variables	Citrate (mmol/L)	Choline (mmol/L)	Cho/Cit (mmol/L)
Healthy tissue TZ, N=221	15.0 [10.5–19.6]	2.5 [2.0–3.0]	0.2 [0.1–0.2]
Tumor TZ, N=15	10.3 [5.4–11.6]	3.1 [2.5–3.5]	0.3 [0.2–0.5]
Healthy tissue PZ, N=222	19.7 [13.2–24.4]	2.4 [1.8–2.9]	0.1 [0.9–0.2]
Tumor PZ, N=182	11.2 [7.1–15.1]	2.7 [2.0–3.3]	0.2 [1.2–0.5]

All values are median [Q1–Q3]. TZ, transition zone; PZ, peripheral zone.

© Quantitative Imaging in Medicine and Surgery. All rights reserved.
https://dx.doi.org/10.21037/qims-22-184